

# Zero kinetic energy photoelectron spectroscopic investigations of hydroquinone isomers

S. CHAKRABORTY, N. BISWAS<sup>#</sup> AND S. WATEGAONKAR<sup>\*</sup>

Department of Chemical Sciences, Tata Institute of Fundamental Research, Colaba, Mumbai 400 005, India.  
email: sanwat@tifr.res.in

Received on July 29, 2005; Revised September 30, 2005.

## Abstract

In this paper, we characterize the vibrational levels of the *cis* and *trans* isomers of hydroquinone (HYQ) cations and determine their adiabatic ionization potentials (IP) using zero kinetic energy (ZEKE) photoelectron spectroscopy. The Franck–Condon activity was observed in the modes 1, 3, 6a, 6b, 9a, 9b, 15 for both the isomers. For a few modes such as 15, 9b, and 6b, the assignments were justified based on the symmetry arguments. The IPs for the *cis* and *trans* isomers were determined to be 64055 and 64008 cm<sup>-1</sup>, respectively. The energy minimized structures and the normal mode frequencies for both the isomers in the cationic ground state ( $D_0$ ) and ground electronic state ( $S_0$ ) were calculated *ab initio* at various levels with the 6-31G\*\* basis set. The optimized energies and frequencies of normal modes for the two isomers in the first electronic excited state ( $S_1$ ) were calculated at the configuration interaction with singlet excitation (CIS) and CASSCF level using the same basis set.

**Keywords:** Hydroquinone isomers, ionization potential.

## 1. Introduction

Hydroquinone (HYQ) is a very interesting molecule. It has two polar hydroxyl groups in *para* position to each other and exists as *cis* and *trans* isomer which marginally differ in their energies. The molecular structure of both the isomers is well known [1]. Microwave spectroscopic [2] data clearly indicates that these two conformers are planar with the two OH groups pointing in the same direction in the *cis* and in the opposite directions in the *trans* isomer. In the ground state, the *trans* form is more stable than the *cis* isomer [3]. Due to the presence of the two polar groups it can form a giant hydrogen bonding network in the solid state giving rise to a well-ordered crystalline structure [4]. In the gas phase it forms homodimers [5] and also the hydrogen-bonded complexes with the polar solvent molecules [6]. The H-bonded complexes with the water molecule have been reported where the OH group acts as a proton donor [6]. The geometry and the vibrational levels of the two isomers of HYQ in the ground state ( $S_0$ ) and first electronic excited state ( $S_1$ ) have been extensively studied and the results indicate that both the conformers show similar Franck–Condon (FC) activity for most of the normal modes in the  $S_1$ – $S_0$  excitation spectrum [7]. It is of interest to know the vibronic structure in the cationic state of HYQ is because the molecule is

\*Author for correspondence.

<sup>#</sup>Present address: Radiation and Photochemistry Division, Bhabha Atomic Research Centre (BARC), Mumbai 400 085, India.

strongly involved in the electrostatic hydrogen bonding interaction which is known to be much stronger in the cationic state.

Müller–Dethlefs and coworkers have pioneered a technique called zero kinetic energy (ZEKE) photoelectron spectroscopy [8, 9] for the vibrational-level characterization of the polyatomic cations like benzene [10] and its derivatives [11]. The basic principle is very simple. At each instance whenever the ionization source is in resonance with one of the internal levels of the cation, there exists a finite probability for the electrons to be formed with zero kinetic energy, in addition to the other channel such as internally cold cation with electrons carrying all the excess energy as the kinetic energy. Therefore if one can discriminate the ZEKE electrons from the prompt electrons it will be possible to study the vibronic spectroscopy of the cations with as good resolution as the  $S_1$ – $S_0$  excitation spectroscopy. Another variance of this technique is the mass-analyzed threshold ionization (MATI) spectroscopy in which case one detects the cations instead of electrons under similar conditions. In principle, MATI and ZEKE give the same spectrum, but the higher voltages applied in the MATI spectrum lead to disadvantages in terms of both optical resolution and signal-to-noise (S/N) ratio [12]. Hence in the case of systems where affirmative mass information is needed MATI would be a better technique than ZEKE. In situations where the mass identification is not very critical and the molecular beam is fairly monomeric such as the case here, the electron detection may have advantage over the cation detection in terms of both achieving higher optical resolution and good S/N ratio.

In this paper, we report the vibronic spectroscopy of the cationic ground state of the two conformers of HYQ using ZEKE spectroscopic technique. Resonance energy photons were used for the excitation of a specific isomer in a specific intermediate vibrational level in the  $S_1$  state and ionization laser was scanned to obtain the ZEKE spectra of the two conformers. Two different intermediate levels were excited to determine the vibrational coupling among the normal modes and to determine the relative geometry changes between the  $S_1$  and  $D_0$  state. MATI spectroscopy of HYQ in the cationic ground state ( $D_0$ ) reported recently [13,14] shows differences in the FC activity of a few normal modes in the two conformers [13]. Our results agree with those reported earlier and in addition a few more vibronic levels were observed due to the inherent greater sensitivity of the ZEKE technique. In a few cases, the normal mode assignments were also revised. The experimental observations were corroborated using the *ab initio* calculations at the level of 6-31G\*\* basis set using the HF/DFT/MP2 level in regard to the vibrational levels and the first ionization potentials (IP) of both the isomers. In addition, CIS and CASSCF calculations were performed to determine the  $S_1$ – $S_0$  excitation energy and the IP.

## 2. Experimental details

The experimental setup, the details of which have been described elsewhere [5] consisted of two 10" diameter differentially pumped stainless steel chambers. A 100  $\mu\text{m}$  pulsed nozzle (General Valve, series 9) housed in the first chamber was used to generate a cold beam of molecules which was collimated before the second chamber by means of a 2-mm skimmer located  $\sim 25$  mm downstream from the nozzle orifice. The time of flight mass spectrometer (TOFMS) with a 20-cm flight tube with a *mu* metal shield was housed in the second cham-

ber. A 10-mm dia channeltron (Philips X919AL) was used to detect the electrons. The output of the channeltron was sent to a digitizing storage oscilloscope (DSO) (Lecroy 9450) and was analyzed by a home-made program.

For the ZEKE experiments (two colour, two photon, using pulsed field ionization), a 10-Hz nanosecond  $\text{Nd}^{+3} : \text{YAG}$  (Quantel Brilliant) laser pumped dye laser (Molelectron DL18P) was used to provide the fixed  $S_1-S_0$  excitation source and another  $\text{Nd}^{+3} : \text{YAG}$  (Quantel YG781C) laser pumped dye laser (Quantel TDL70) was used to provide the tunable  $D_0-S_1$  ionization source. The two co-propagating beams were spatially and temporally overlapped and were focused on to the molecular beam using a 1-m focal length lens. The two beams intersected the skimmed molecular beam at 70 mm downstream from the skimmer. The line width of the Quantel dye laser was  $0.08 \text{ cm}^{-1}$  and that of the Molelectron dye laser was  $0.3 \text{ cm}^{-1}$ . Typical pulse energies were  $\sim 5-10 \mu\text{J}$  for the excitation laser and  $\sim 100 \mu\text{J}$  for the ionization laser. Excitation pulse energy was maintained low enough to avoid the space charge effects of excessive ionization due to two photon absorption at the excitation wavelength. The ZEKE spectra were recorded using two intermediate levels, viz. the band origin (BO) and the  $6a$  ( $v = 1$ ) level of the  $S_1$  for both the *cis* and *trans* isomers. The ionization laser was scanned between  $30015$  and  $31900 \text{ cm}^{-1}$  using the frequency-doubled output of a mixture of DCM and LDS698 dyes (Exciton Inc.). The dye laser was calibrated by means of the opto-galvanic method using an Fe–Ne hollow cathode lamp.

The ZEKE experiments were carried out in the Wiley–McLaren [15]-type TOFMS using the following pulse sequence for improving the S/N ratio. Initially, both the extraction (bottom) and the acceleration (middle) grids (separated by 32 mm) were held at the same voltage of  $\sim -60 \text{ V}$  with a spoil field of about  $500 \text{ mV/cm}$  between the two grids so that ionization occurs under near-field free condition. The third grid situated above the middle grid is electrically grounded so that the electrons drift to the detector in the field-free region. A few nanoseconds, typically  $\sim 500 \text{ ns}$  (SRS; DG-535), after the ionization laser pulse, the bottom grid is pulsed (made more  $-ve$  relative to the middle grid) such that the effective extraction field was  $6 \text{ V/cm}$  for the duration of  $2 \mu\text{s}$ . This allows one to extract the ZEKE electrons at very low electric fields and then accelerate them towards the detector using higher acceleration field ( $\sim 40 \text{ V/cm}$ ) thereby increasing the collection efficiency at the detector.

Hydroquinone is a solid at room temperature. It was heated to about  $125^\circ\text{C}$  to generate sufficient amount of vapor pressure to record spectrum with good S/N ratio. It was purchased from S. D. Fine Chemicals Ltd and used without further purification. Helium, obtained from local commercial sources, was used without further purification as the buffer gas. The typical backing pressure was  $\sim 2 \text{ atm}$ . The typical working pressure in the source chamber was  $\sim 2 \times 10^{-5} \text{ torr}$  and in the TOFMS chamber  $\sim 2 \times 10^{-6} \text{ torr}$ .

### 3. Computational details

*Ab initio* quantum chemical calculations were performed using the Gaussian 98 program package [16]. The Hartree–Fock (HF), Møller–Plesset perturbation of second-order (MP2), Density Functional Theory (DFT) methods using 6-31G\*\* basis set were used to obtain the optimized structures, total energies, and normal mode frequencies for both conformers in

the  $S_0$  and  $D_0$  states. The configuration interaction singles (CIS) method was applied to obtain the excited state energies and frequencies. The ionization potentials were obtained as the difference between the optimized energies of the ground state ( $S_0$ ) and the cationic ground state ( $D_0$ ). Zero point energy correction (ZPE) was incorporated to obtain more accurate result. The IP and the  $S_1$ - $S_0$  excitation energy was also calculated using the complete active space self-consistent field (CASSCF) method. The CASSCF calculations were carried out with ten electrons in eight orbitals (10, 8) active space for the ground state ( $S_0$ ) and the first electronic excited state ( $S_1$ ), and with nine electrons in eight-orbital (9, 8) active space for the cationic ground state ( $D_0$ ). These eight orbitals include all five occupied and the three lowest unoccupied  $p$  orbitals.

#### 4. Results and discussion

The  $S_1$ - $S_0$  electronic excitation spectrum of HYQ reported in the literature [7] shows that the vibronic features in the spectrum appear in two series built on the band origins at 33508 and 33540  $\text{cm}^{-1}$ , corresponding to the *trans* and *cis* isomers, respectively. The excitation laser was tuned to either of these two energies and the photo ionization efficiency curves were initially recorded to determine the ionization threshold of the two species using DC extraction field. Then the region around the ionization threshold was scanned using the pulsed field ionization to determine the adiabatic ionization potential and record the ZEKE spectra. Figure 1 displays the pulsed field-ionized ZEKE spectra of *trans*-HYQ recorded by ionization via the band origin (33508  $\text{cm}^{-1}$ ) and the  $6a^1$  (33949  $\text{cm}^{-1}$ ) excitation in the  $S_1$  state. The strongest peak in the spectrum appears at 30500  $\text{cm}^{-1}$  which gives the field-corrected adiabatic ionization potential (IP) of *trans*-HYQ as  $64011 \pm 5 \text{ cm}^{-1}$ .

The spectral features observed in the spectrum are due to various vibrational levels of the cations. Besides the band origin of the cation, the spectrum shows two strong transitions at 31343 and 31679  $\text{cm}^{-1}$  along with several weak transitions which are shown as the expanded inset in the figure. These two transitions were assigned to mode 1 and mode 9a. Varsanyi's nomenclature [17] was followed for the normal mode assignments. The assignments to the spectral features were guided by symmetry considerations, experimental values available for the corresponding mode in the  $S_0$  and  $S_1$  states, and using the normal mode frequencies calculated using 6-31G\*\* basis set at the DFT level employing B3LYP functional. The other observed transitions are listed in Table I along with the possible assignments and the *ab initio* computed normal mode frequencies. The FC activity was mainly observed in modes 6a, 9a, 15, 9b, 6b, and 1, which are depicted in Fig. 2.

Figure 1(b) shows the ZEKE spectrum recorded via the  $6a^1$  intermediate  $S_1$  vibronic level. The lowest energy transition matches with the band origin of the cation and the strongest transition observed at 458  $\text{cm}^{-1}$  from the band origin was assigned as the  $\Delta v = 0$  transition in the 6a mode and gives the frequency of the 6a mode as 458  $\text{cm}^{-1}$ . This coincides with the higher energy transition of the doublet observed at  $\sim 460 \text{ cm}^{-1}$  in the spectrum shown in Fig. 1(a).

Figure 3 displays the ZEKE spectrum of *cis*-HYQ recorded via the band origin (33540  $\text{cm}^{-1}$ ) and the  $6a^1$  (33980  $\text{cm}^{-1}$ ) vibrational level of the  $S_1$  state. The field-corrected adiabatic IP of *cis*-HYQ was found as  $64058 \pm 5 \text{ cm}^{-1}$ , which is 47  $\text{cm}^{-1}$  higher than that of

**Table I**  
**Observed transitions ( $\text{cm}^{-1}$ ) in the ZEKE spectra of *trans* and *cis* isomers of HYQ and their assignments<sup>a</sup>**

<i>trans</i> Isomer		Calc. freq.	<i>cis</i> Isomer		Calc. freq.	Mode assignment <sup>b</sup>
Intermediate level in $S_1$ state	$6a^1$		Intermediate level in $S_1$ state	$6a^1$		
$0^0$			$0^0$			
365 (vw)	363 (vw)	365	365 (m)	367 (w)	366	$15^1$ (365)
443 (w)		447				$9b^1$ (439)
458 (w)	457 (vs)	465	459 (m)	457 (vs)	465	$6a^1$ (459/456)
			521 (vw)			$16b^1$
			550 (vw)			OH op sym bend
566 (vw)			562 (vw)			OH op asym bend
611 (w)		624		673 (w)		$6b^1$
						Unassigned
729 (vw)			728 (m)			$15^2$
	821 (w)			822 (m)		$6a^1 + 15^1$
843 (s)		853	839 (s)	838 (w)	852	$1^1$ (837/834)
	903 (w)					$6a^1 + 9b^1$
918 (w)	916 (m)		919 (vw)	916 (m)		$6a^2$
972 (w)	973 (vw)		986 (vw)			$15^1 + 6b^1$
	1072 (w)					$6a^1 + 6b^1$
			1099 (vw)			$15^3$
1179 (s)	1176 (w)	1199	1178 (s)	1172 (w)	1202	$9a^1$ (1175/1174)
	1186 (w)			1186 (w)		$6a^1 + 15^2$
1210 (vw)			1209 (m)			$1^1 + 15^1$
			1286 (w)			$6a^2 + 15^1$
1294	1294 (s)			1294 (s)		$6a_1^1 + 1_0^1$
1333						$15^2 + 6b^1$
1342		1364				$3^1$ (CH ip bend)
	1429					$6a^1 + 15^1 + 6b^1$
				1378 (w)		$6a_1^3$
	1632 (s)			1634 (s)		$6a^1 + 9a^1$
	1661 (w)			1659 (m)		$6a^1 + 1^1 + 15^1$

<sup>a</sup>The observed values are given with respect to the band origin of the *trans* and *cis* isomers at 30,500 and 30,515  $\text{cm}^{-1}$ , respectively. Theoretical values were calculated at the DFT level using the B3-LYP functional and 6-31G\*\* basis set. Relative intensity of the peaks was also given in the parentheses; vw = very weak, w = weak, m = medium, s = strong, and vs = very strong.

<sup>b</sup>Numbers in parentheses are from Ref. 13 given as (*trans/cis*).

the *trans*-HYQ. The FC activity observed in this BO excited spectrum is distinctly different (note the factor of 2 difference between the expansion factors used for the insets in Figs 1 and 3) than that of the *trans* isomer, *vide infra*. The spectrum recorded via the  $6a$  intermediate level (Fig. 3b) shows similar FC activity as that of the *trans* isomer in regard to the  $\Delta v = 0$  transition of the  $6a$  mode. The observed transitions are reported in Table I along with their assignments. The ionization potentials determined in this work are in excellent agreement with the values of 63998/64051  $\text{cm}^{-1}$  [13] and 63999/64054  $\text{cm}^{-1}$  [14] reported previously for the *trans/cis* isomers, respectively.

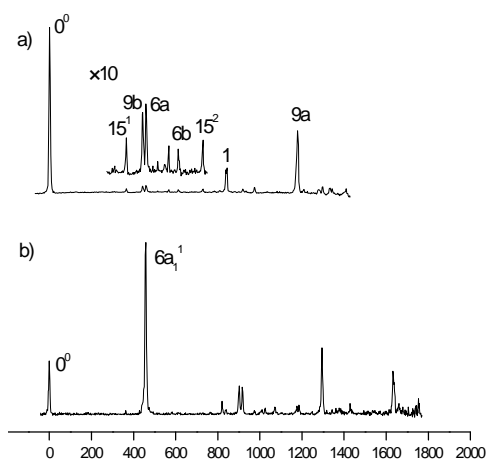


FIG. 1. ZEKE spectra of *trans*-HYQ, recorded via (a) the  $S_1$   $0^0$  ( $33508\text{ cm}^{-1}$ ) and (b) the  $S_1$   $6a^1$  ( $33949\text{ cm}^{-1}$ ) intermediate states. Traces are plotted with respect to the origin of the  $D_0$ - $S_1$  spectrum at  $30500\text{ cm}^{-1}$ . The inset in (a) is expanded 10 times.

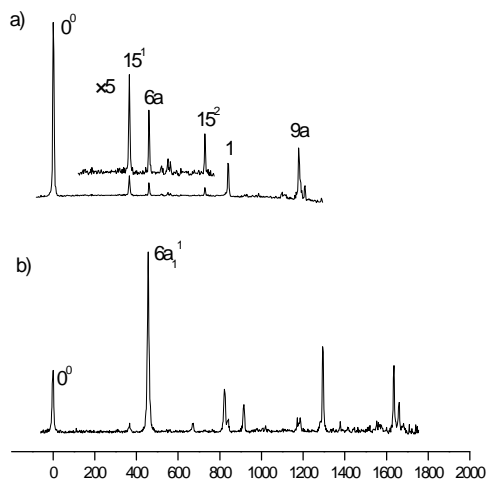


FIG. 3. ZEKE spectra of *cis*-HYQ, recorded via (a) the  $S_1$   $0^0$  ( $33540\text{ cm}^{-1}$ ) and (b) the  $S_1$   $6a^1$  ( $33980\text{ cm}^{-1}$ ) intermediate states. Traces are plotted with respect to the origin of the  $D_0$ - $S_1$  spectrum at  $30515\text{ cm}^{-1}$ . The inset in (a) is expanded five times.

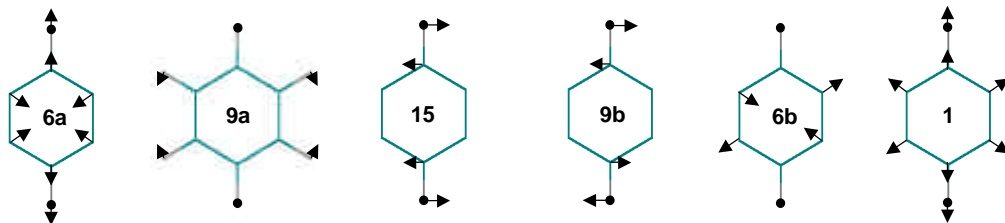


FIG. 2. Vibrational displacements vectors of observed modes.

The observed FC activity in the  $6a$  mode in both the *trans* and *cis* spectra indicates two things. First, the  $\Delta v = 0$  transition is the strongest in both the isomers and second, there is hardly any progression in this mode, i.e. the intensity steeply decreases for  $\Delta v > 0$ . This is in stark contrast to that observed in the case of  $S_1$ - $S_0$  excitation spectrum [18] where a long progression was observed up to  $v' = 7$ . This observation suggests that the geometry change along the  $6a$  normal mode in the cation relative to the  $S_1$  state is negligible compared to the change in the  $S_1$  state relative to the  $S_0$  state. Secondly, the spectra recorded via the  $6a$  intermediate level appear very similar to that recorded via the BO excitation with the  $6a_1^1$  ( $\Delta v = 0$ ) transition acting as the pseudo origin except that slightly higher FC activity is observed in all the transitions. Especially, the relative intensities of the  $1^1$  and  $9a^1$  transitions are reversed. This indicates that in the cation mode  $6a$  is strongly coupled to mode 1.

The molecular structure of *trans* and *cis* HYQ is well known [1] and microwave spectroscopic [2] data clearly indicates that these two conformers are planar and belong to the point group  $C_{2h}$  and  $C_{2v}$ , respectively. The  $C_2$  axis however is differently oriented in the two

cases; in *trans*-HYQ it is perpendicular to the aromatic plane, whereas in the case of *cis* isomer it lies in the plane of the molecule and bisects the two central CC bonds. This has interesting consequences on the symmetries of certain normal modes. For example, mode 15, which is the in-plane C–O bending mode that is symmetric w.r.t. the CC axis involved in *para* substitution, is totally symmetric ( $a_1$ ) for *cis*-HYQ and nontotally symmetric ( $b_u$ ) for *trans*-HYQ. On the other hand, mode 9b which is the antisymmetric in-plane C–O bending vibration is totally symmetric ( $a_g$ ) for the *trans*-HYQ and vice versa. Another example is that mode 6b, which is one of the in-plane ring deformation modes, is totally symmetric to the *trans* isomer and nontotally symmetric for the *cis* isomer. These facts are reflected very well in the observed spectra. In the *trans*-HYQ spectrum, the transition at  $365\text{ cm}^{-1}$  (which is assigned the  $15^1$  transition) is very weak, whereas the same transition in the *cis*-HYQ spectrum appears very prominently. On the other hand, the transition due to mode 9b (lower energy transition of the doublet at  $460\text{ cm}^{-1}$ ) and 6b ( $611\text{ cm}^{-1}$ ) appears in the *trans* but is totally absent in the case of *cis* isomer. The peak observed at  $\sim 729\text{ cm}^{-1}$  (an overtone of the transition at  $365\text{ cm}^{-1}$ ) with weak to moderate intensity for both the *trans* and *cis* isomers was assigned as the  $15^2$  transition. This peak was assigned to mode 12 by Tzeng and coworkers [13]. We are not very comfortable with this assignment for the following reason. Mode 12 is nontotally symmetric for both the *trans* and *cis* isomers and hence the  $\Delta\nu = 1$  transition would not be an allowed transition. The observed intensity difference in the  $\Delta\nu = 1$  transition at  $365\text{ cm}^{-1}$  of the two isomers and the fact that the  $729\text{ cm}^{-1}$  happens to be an exact overtone, assignment of these two features as  $\Delta\nu = 1$  and 2 transitions of mode 15 is appropriate.

The frequencies of the totally symmetric in-plane ring deformation modes such as the 6a mode ( $457/458\text{ cm}^{-1}$ ) (the two numbers refer to the *trans*- and *cis*-isomers, respectively, throughout this paragraph) and ring-breathing mode 1 ( $843/839\text{ cm}^{-1}$ ) determined in this work can be compared with those in the  $S_1$  and the  $S_0$  states. These were  $441/440$  and  $822/828\text{ cm}^{-1}$  in the  $S_1$  state and  $469/469$  and  $853/852\text{ cm}^{-1}$  in the  $S_0$  state, respectively [18]. Thus the frequencies in the cation are blue-shifted compared to that in the  $S_1$  state by about  $20\text{ cm}^{-1}$  and are red-shifted compared those in the  $S_0$  state. It is a general observation that most of the ring-deformation modes are red-shifted in the  $S_1$  state due to reduction in the pi bond order because the  $S_1$ - $S_0$  transition is a  $p$ - $p^*$  transition. Since the HOMO is the  $p^*$  orbital in the case of  $S_1$  state the first ionization must involve the removal of the  $p^*$  electron, effectively increasing the pi bond order in the cation relative to that in the  $S_1$  state. Therefore, the pi bond order of the aromatic ring is expected to be in the order  $S_0 > D_0 > S_1$ . This is well reflected in the observed frequencies of the 6a and 1 modes. The frequencies of most of the observed modes for the cation for the two isomers are within a few wavenumbers of each other indicating that the relative orientation of the OH groups in the two isomers has no effect on their force fields. This was also found to be true in the  $S_0$  and  $S_1$  states.

The energies of both the isomers of the cation were optimized at the HF, B3LYP, and MP2 level using the 6-31G\*\* basis set. Normal mode calculations at these geometries gave all positive frequencies indicating that these were the most stable structures. At all level of calculations the *trans* isomer was more stable than *cis* one in the  $S_0$ ,  $S_1$ , and  $D_0$  states, except that at the MP2 level the *cis*-HYQ was calculated to be more stable than *trans* isomer in the  $D_0$  state. Experimental results indicate that *trans*-HYQ is stable than the *cis* isomer in

**Table II**  
**Energies of the  $S_0$ ,  $S_1$  and  $D_0$  states of *cis*- and *trans*-HYQ at various levels of calculation using 6-31G\*\* basis set**

Level of calculation	<i>trans</i> -HYQ (cm <sup>-1</sup> )				<i>cis</i> -HYQ (cm <sup>-1</sup> )			
	$S_0$	$S_1$	$D_0$	IP	$S_0$	$S_1$	$D_0$	IP
HF	0	–	52637 (186)	52823	13	–	52839 (172)	52998
DFT	0	–	59271 (279)	59550	31	–	59370 (278)	59617
MP2	0	–	60924 (1762)	62685	28	–	60844 (2388)	63203
CIS	0	44366	–	–	54	44451	–	–
CASSCF	0	36371	55905 (514)	56419	25	36447	56031 (503)	56508

<sup>a</sup>All the energies are given relative to the *trans*-HYQ  $S_0$  state energies, which are –380.4301182, –382.6957666, –381.5764249, –381.5688037, and –380.5031365 for the HF, DFT, MP2, CIS, and CAS, respectively, in Hartrees.

<sup>b</sup>The values in parentheses indicate the  $\Delta ZPE$  between the corresponding state and the  $S_0$  state.

<sup>c</sup>IP is the sum of the  $D_0$  state energy and the  $\Delta ZPE$ .

all the states. In the  $S_1$  state *trans*-HYQ is relatively more stable than the *cis* by 32 cm<sup>-1</sup> whereas in the  $D_0$  state *trans* is found to be more stable by 47 cm<sup>-1</sup>. This indicates that there must be some apparent differences in the *trans* and *cis* electronic structures which makes the MP2 calculations account for the electronic correlations quite differently for the two isomers in the  $D_0$  state. This is also apparent in the fact that the strength of coupling between the two OH oscillators was quite different in the two isomers, i.e. the difference in the symmetric and antisymmetric OH stretching frequencies for the *trans* isomer was 491 cm<sup>-1</sup> compared to 1369 cm<sup>-1</sup> for the *cis* isomer indicating much stronger coupling in the latter. The extent of coupling of the two OH oscillators predicted at the MP2 level is clearly unrealistic. At all other levels of calculations, the frequencies of the two modes differ barely by 10 to 20 cm<sup>-1</sup>. The adiabatic IPs of the *trans* and *cis* isomers were determined as 64011 ± 5 and 64058 ± 5 cm<sup>-1</sup>, respectively, in this work. The IPs calculated at the MP2 level are in excellent agreement with the experimental values among the three levels of calculations (Table II). The error in the IP values at the CASSCF level was larger than the MP2 and DFT values indicating that the choice of the orbitals included in the complete active space was clearly inadequate. Some more work in this area is needed.

## 5. Conclusions

The vibronic levels of jet-cooled HYQ cations were investigated using pulsed field-ionized ZEKE spectroscopy. The adiabatic ionization potentials of the *trans* and *cis* isomers of the HYQ were determined as 64011 ± 5 and 64058 ± 5 cm<sup>-1</sup>, respectively, which are in excellent agreement with those reported earlier. The FC activity in the ZEKE spectra was mainly observed in the totally symmetric 6a, 9a, and 1 modes. Other observed modes gave an excellent manifestation of the symmetry principles dictating their appearances in the spectra. Mode 15 was observed very prominently in the case of the *cis* isomer whereas modes 6b



and 9b were found to be active only in the case of *trans*-HYQ. All of the observed normal modes were blue-shifted relative to that in  $S_1$  state but were red-shifted w.r.t. the ground state. This suggests that the pi bond order of the aromatic ring in the  $D_0$  state was intermediate between the  $S_0$  and the  $S_1$  states. *Ab initio* calculations at all the levels except the MP2 level predicted correctly the order of stability of the two isomers in all the states. At the MP2 level the order was reversed in the  $D_0$  state. The calculated IP at the MP2 level was the most accurate i.e. within 2% of the experimentally determined values.

## References

1. S. J. Humphrey, and D. W. Pratt, High resolution  $S_1 \leftarrow S_0$  fluorescence excitation spectra of hydroquinone. Distinguishing the *cis* and *trans* rotamers by their nuclear spin statistical weights, *J. Chem. Phys.*, **99**, 5078–5086 (1986).
2. W. Caminati, S. Melandri, and L. B. Favero, Microwave spectroscopy of hydroquinone: The rotational spectrum of the *cis* conformer, *J. Chem. Phys.*, **100**, 8569–8572 (1994).
3. A. Oikawa, H. Abe, N. Mikami, and M. Ito, Electronic spectra and ionization potentials of rotational isomers of several disubstituted benzenes, *Chem. Phys. Lett.*, **116**, 50–54 (1985).
4. J. L. Atwood, J. E. D. Davies, and D. D. MacNicol (eds) *Inclusion compounds*, Academic Press, Vols 1–3, (1984); G. R. Desiraju, *Angew. Chem. Int. Ed. Engl.*, **34**, 2311– (1995).
5. N. Biswas, S. Chakraborty, and S. Wategaonkar, Gas phase spectroscopic studies of hydroquinone dimer, *J. Phys. Chem. A*, **108**, 9074–9081 (2004).
6. P. S. Meenakshi, N. Biswas, and S. Wategonkar, Gas phase spectroscopic studies on hydroquinone–water complex, *Phys. Chem. Chem. Phys.*, **5**, 294–299 (2003).
7. G. N. Patwari, S. Doraiswamy, and S. Wategaonkar, Hole-burning spectroscopy of jet-cooled hydroquinone, *Chem. Phys. Lett.*, **289**, 8–12 (1998).
8. Klaus Müller-Dethlefs, and Edward W. Schlag, High-resolution zero kinetic energy (ZEKE) photoelectron spectroscopy of molecular systems, *A. Rev. Phys. Chem.*, **42**, 109–136 (1991).
9. E. W. Schlag, *ZEKE spectroscopy*, Cambridge University Press (1998).
10. L. A. Chewter, M. Sander, K. Müller-Dethlefs, and E. W. Schlag, High resolution zero kinetic energy photoelectron spectroscopy of benzene and determination of the ionization potential, *J. Chem. Phys.*, **86**, 4737–4744 (1987).
11. D. Rieger, G. Reiser, K. Müller-Dethlefs, and E. W. Schlag, Zero kinetic photoelectron spectroscopy of *p*-difluorobenzene, *J. Phys. Chem.*, **96**, 12–14 (1992).
12. L. Zhu and P. Johnson, Mass analyzed threshold ionization spectroscopy, *J. Chem. Phys.*, **94**, 5769–5771 (1991).
13. J. L. Lin, L. C. L. Huang, and W. B. Tzeng, Mass-analyzed threshold ionization spectroscopy of the selected rotamers of hydroquinone and *p*-dimethoxy benzene cations, *J. Phys. Chem. A*, **105**, 11455–11461 (2001).
14. M. Gerhards, C. Unterberg, and S. Schumm, Structure and vibrations of dihydroxybenzene cations and ionization potentials of dihydroxybenzenes studied by mass analyzed threshold ionization and infrared photoinduced Rydberg ionization spectroscopy as well as *ab initio* theory, *J. Chem. Phys.*, **111**, 7966–7975 (1999).
15. W. C. Wiley, and I. H. McLaren, Time-of-flight mass spectrometer with improved resolution, *Rev. Sci. Instrum.*, **26**, 1150–1157 (1955).
16. M. J. Frisch *et al.*, *Gaussian 98*, revision A.11.2, Gaussian, Inc., Pittsburgh, PA (2002).
17. G. Varsanyi, *Assignment of vibrational spectra of 700 benzene derivatives*, Vol. 1, Wiley (1974).
18. G. N. Patwari, S. Doraiswamy, and S. Wategaonkar, Spectroscopy and IVR in the  $S_1$  state-of-jet-cooled *p*-alkoxyphenols, *J. Phys. Chem. A*, **104**, 8466–8474 (2000).